Grain Size Distribution and Sediment Flux Structure in a River Profile, Measured with a LISST-SL Instrument

Yogesh.C. Agrawal, Ole A. Mikkelsen and H. C. Pottsmith[1]

Abstract

New data on sediment transport in a river are reported using a LISST-SL laser diffraction instrument that simultaneously measures velocity, optical transmission, depth, temperature, and sediment particle size distribution (PSD) isokinetically. Suspended sediment concentration (SSC)is obtained from the sum of PSD. Optical transmission is seen to be nearly constant in the top 3.5m of the 4m deep river. The PSD profile, however, reveals a vertically well-mixed wash load, seen by the transmissometer, plus a coarse grain (>63μm) mode that increases in size and concentration towards the riverbed, but which is not seen by the transmissometer. The insensitivity of transmission to coarse particles is similar to turbidity data reported by Orton & Kineke 2001, and Laguionie et al., 2007. They also did not see the coarse particle mode except very close to the riverbed (0-0.1 depth). The present data show downward increasing sediment concentration and flux of coarse grains, beginning right near the surface. Near the bed, the sediment flux and concentration of coarse grains are, respectively, factors 3 and 2 higher than at the surface. The slopes of concentration profiles of different particle sizes follow Rouse (1937) closely, and are sufficiently ordered to provide consistent estimates of the friction velocity u_* in the water column. SSC statistics from 0.5 to 3.5m show skewness due to the minimum concentration imposed by washload, implying potential for bias in sampling. The mass mean sediment diameter is seen to increase by a factor of 5 from surface to bottom. The apparent insensitivity of the transmissometer is explained by a factor 2.5 increase in Sauter Mean Diameter (particle volume/area) from top to near-bottom. Finally, it is seen that a mean velocity and SSC estimate at half-depth is within experimental error of column-mean values. However, PSD at half-depth is not representative of the column mean PSD.

Keywords: sediment transport, rivers, LISST-SL, sediment flux, vertical structure.

Introduction

Sediment transport in rivers has important societal consequences; as such it is a subject of significant scientific research. River meander, sand formations, erosion around bridge pilings, and discharges into estuaries and deltas are all related subjects. The effort in measuring suspended and bedload discharge has a long history (see Orton and Kineke, 2001 for a review; also Kazimierz et al. 2010). Routine monitoring by governments have evolved rigorous procedures and standardized instruments and methods. The present work confirms some old ideas, and advances others.

[1] Sequoia Scientific, Inc., 2700 Richards Rd, Bellevue, WA 98005, USA

The simplest study areas on rivers are straight sections which are devoid of secondary motions associated with river meanders. Barring complex bed topography, this is describable, to first order, as a classic flow in a turbulent channel (Schlichting,1968). In these flows, a 'law of the wall' region exists near the riverbed, where the velocity profile scales as logarithm of the distance from the bed. Such a region exists so long as the channel bed roughness is not a significant portion of the channel depth. Above this logarithmic velocity region, a 'law of the wake' applies where scaling is with channel depth. In these flows, sediment is carried both as suspended load and as bedload. The suspended load carried by rivers can typically be partitioned into a 'wash load' of fine material that is too fine to settle and a resuspended load if the river velocity is sufficient to force resuspension. A vertical gradient in suspended sediment concentration (SSC) exists in the water column. The gradient is established as the competing action of turbulent diffusion, which tries to mix sediments throughout the water column, is countered by gravitational settling. Since gravitational settling velocity depends on grain size and mass density, size determines the gradient – faster settling sediments exhibit stronger gradients, and vice versa. This was formalized by Rouse (1937). Thus, river channels are expected to exhibit velocity and SSC profiles with scaling laws similar to classic turbulent channels. The SSC profiles are expected to be a composite of component profiles of different size sediments (modified by sediment-induced density stratification when it exists). It is this last item – gradients of different sized grains – that have remained poorly studied, and remain a source of error and disorder in past data because of instrumental limitations to observe size distributions and accurate sediment concentrations.

Orton and Kineke (2001) measured velocities and sediments in the Hudson River estuary and compared model results with measurements. Their sediment sensor was the OBS optical turbidity sensor, which provides an area-based measurement (i.e. it calibrates to particle area concentration, not volume or mass). They used a single calibration of the OBS, by implication, assuming a constant size distribution throughout the water column. OBS sensors provide no information on particle grain size. With no data on size distribution variability in the water column, they assumed a single settling velocity for their model, 0.22cm/s, which applies to 50 μm sand grains. They reported that the theory-data match was best when a power law relationship was employed between settling velocity and concentration. When they inverted their data assuming Rouse profile, they found an order of magnitude variability in the concentration-settling velocity relationship. This is, of course, highly unsatisfactory and the assumption of a relationship between concentration and settling velocity is poorly grounded in physics. Even so, data and their models disagreed by orders of magnitude at just short distances above the riverbed. In the end, the use of turbidity type sensors appears to have been unsuitable in this vertically changing PSD environment. It appears to be responsible, at least in part, for the poor match between data and their sophisticated models.

A similar issue regarding sediment data can be found in the later work of Laguionie et al.(2007) who studied velocity and SSC profiles in the Vilaine river in the Brittany region of France. Their data has good velocity characterization, but suffers in the correct description of sediment concentration distribution again due to the use of turbidity meters. They reported a nearly constant SSC in normalized depth from 0.1 to 1. Only below a normalized depth of 0.1 was a steep turbidity gradient seen. In contrast, the present data reveal a gradient in concentration filling the full depth of the river.

Still other studies have employed physical samples. An example of this is the work of Richey et al.(1986). They employed bag samplers and partitioned a vertically integrated sample into two size classes: fine and coarse, with the break at 63 μm. These data are more likely to be accurate, but for sampling errors. Unfortunately, this limits the number of available data points, and vertical structure of PSD was not revealed.

The new data in the present paper arise from the use of new technology, namely laser diffraction (LD). LD permits measurement of size distribution, and from that, with assumed mass density, mass concentration, or SSC, by summation. The calibration of such an instrument is constant no matter the sediment grain size, so long as the grains are within the measurable size range of the instrument. These size ranges are usually quite broad, e.g. in the present instance, the covered sizes range from 2 to 400 microns. The limitation of turbidity meters, in contrast, is that they measure particle area concentration (particle area per unit volume of water), not volume or mass concentration (μl/L, or mg/L). The sensitivity to grain color and the $1/d$ dependence of sensitivity to grain diameter, d is well-known, reported by Sutherland et al. (2000) and others. Acoustic backscatter sensors are also in use, though mostly qualitatively. Acoustics also respond to quantities other than particle volume or mass concentration of suspended sediments, and are subject to similar limitations (Hanes and Thorne, 2002).

The LD method is an international standard, ISO-13320:2009. Laboratory LD instruments have been available for over 3 decades that employ this method to construct only PSD, without emphasis on SSC. The LISST-SL is a new laser diffraction instrument, developed in the course of a Cooperative Research and Development Agreement (CRADA) between Sequoia Scientific, Inc. of Bellevue, Washington and the United States Geological Survey[2] (USGS). This instrument measures PSD, SSC, velocity, temperature, optical transmission, and depth. From this complete set of data from the Cowlitz river in Washington State, we report new findings. The data reveal a vertically well-mixed wash load centered at a grain size of ~6ϕ, and a resuspended load with a strong vertical gradient throughout the full water column. The data also reveal that the gradients in concentrations are steeper for coarser grains, following Rouse-like predictions. The mix of wash-load and resuspended load produces the distribution of concentration to be statistically skewed. The skewness can affect measurement accuracy of physical samplers.

[2] The CRADA does not imply an endorsement of the instrument by USGS.

We are examining precisely the same questions addressed by Laguionie et al.(2007) and Orton and Kineke(2001) – the vertical profile of velocity and suspended sediments. Additionally, we examine if water-column mean velocity, SSC, and PSD are reasonably accurately measured with a single measurement at a fixed depth (e.g. 60% of depth), as is common practice. The results are of significance to to everybody concerned with measuring SSC flux in rivers: researchers, consultants and monitoring agencies.

Instrumentation

Laser Diffraction Review: A collimated laser beam illuminates particles in water, Fig.1a. Light scattered by particles into small forward angles is collected by a lens. A specially constructed silicon detector array is placed at the focal plane of this lens. The detector array consists of a set of concentric rings of silicon. Each detector ring senses light scattered into a small range of specific angles from the laser beam. At the center of the rings, a small, 75μm diameter hole permits passage of the focused laser beam, which is detected by a photodiode placed behind the ring detector. This latter measurement, when normalized by its value for particle-free water, provides a measure of beam attenuation. The beam attenuation, like turbidity, is directly proportional to the particle area concentration and therefore is not usable as an indication of SSC. Instead, it is merely used to de-attenuate scattered light reaching ring

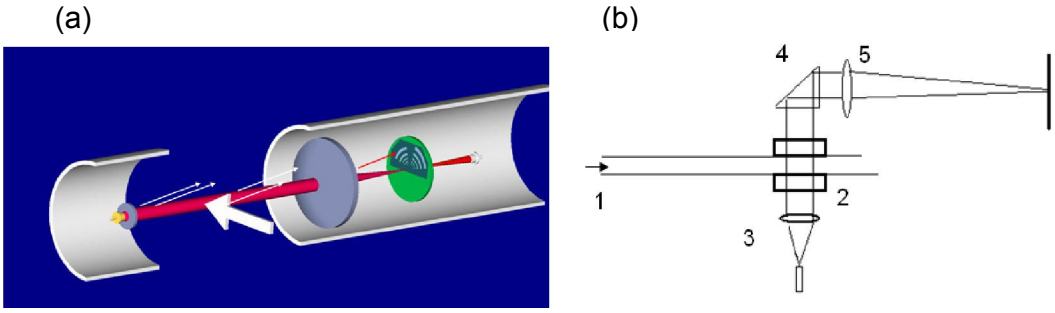

Figure 1: (*a*) Optics of laser diffraction, simplified, (*b*) actual in the LISST-SL; 1- water intake; 2 – optical windows; 3 – collimating lens; 4- laser folding prism; 5 – focusing lens.

detectors, which is equally attenuated. The beam attenuation is saved in the data file.. The dynamic range of sizes measurable with LD (maximum to minimum diameter ratio) is determined by the ratio of the largest to smallest radii of detector rings. The range of particle concentrations that can be measured is defined at the low end from the sensitivity of scattered light detectors, and on the upper end, by the onset of significant multiple scattering (light re-scattered after being scattered once). Optical transmission is a good indicator of multiple scattering. We use 30% transmission value to define the upper concentration limit. Since transmission depends on particle area concentration, this transmission corresponds to a size-dependent limit on upper concentration. Following Agrawal et al.(2008), the upper working limit is

specifiable as *d/L* mg/L, where *d* is grain diameter (μm), and *L* is the path length (m) of the laser beam in turbid water.

The LISST-SL Instrument: The LISST-SL instrument, manufactured by the authors' company is shown in cross-section in Fig.2, and assembled in the inset. It uses folded-path optics, Fig.1b. To accommodate the high concentrations that occur in rivers, the path length is kept short, *L*=0.003m. Consequently, for 10 μm grains, the upper limit of operation is 3,300 mg/L. For 100 μm grains, the limit is 33g/L. For a distribution of sizes in suspension, the relevant diameter is the Sauter Mean diameter (ratio of total volume to total particle area).

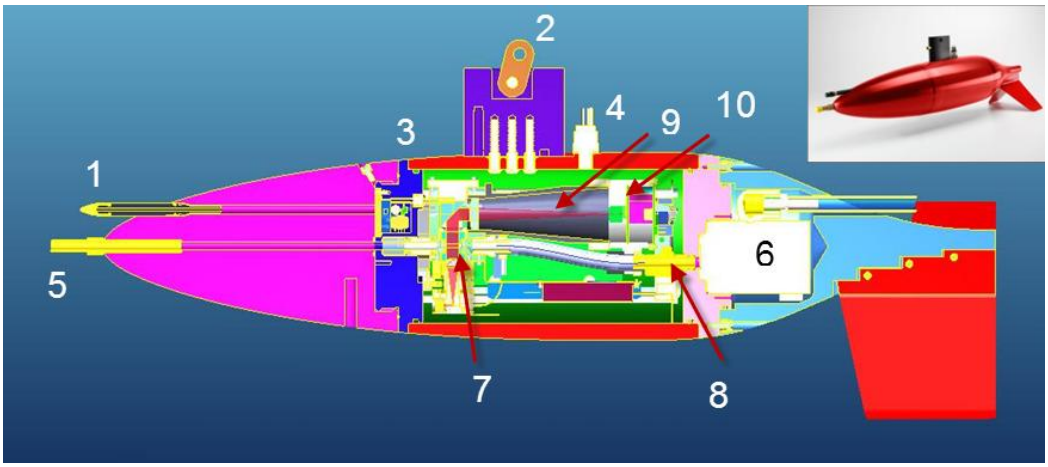

Figure 2: The LISST-SL instrument in cross-section. 1:pitot tube; 2-lifting point, 3- static port; 4 underwater connector; 5- water intake; 6- intake assist pump; and 7 – laser beam at measurement volume; 8- temp sensor; 9- scattered light path; and 10-ring detector (seen edge-on).

The body shape is a low-drag form derived from Parsons et al.(1975). It is comprised of 3 sections: nose, middle, and tail. The nose section holds an intake tube and a pitot tube. Impact pressure sensed with the pitot tube is saved as a measure of velocity, and it is used to control the intake-assist pump, located in the tail section, to achieve and maintain isokinetic withdrawal. Particular care has been taken to minimize drift in the pitot impact pressure sensor. The instrument is lowered by a 2-conductor wire from a cableway or a bridge using a USGS B-reel. Power supply to the instrument and communication with the instrument is also done using the same 2-conductor wire. While one end of this wire attaches to the lifting point on the instrument, the other end connects to a Topside Control Box (TCB), which contains control electronics, display and battery (see below). Additional weights can be attached to the instrument for working in deep or swift rivers.

The LISST-SL mid-section contains the optics and electronics, Fig.2. The laser is a 670nm fiber-coupled device, collimated by a 20mm focal length lens. The 4 mm diameter collimated beam crosses the measurement section, which is rectangular, sized 3 mm x 20 mm. The laser beam and scattered light

are then folded by a 45-degree prism (see also Fig.3*b*), to direct light to the ring detectors. The sediment measurement section is in the mid-section of the streamlined body, mounted on a bulkhead, and connecting the straight axial intake in the nose section. Water exits the measurement section through a stiff Teflon tube within the center section. This tube connects to the pump through a metal fitting, into which a thermistor is installed to sense water temperature. Amplifiers for the ring detectors, signal transmission electronics, and pump controller are placed within the mid-section. Power and signals travel on a common 2-conductor wire which is also used to suspend the instrument into the river. The TCB contains the battery and instrument control electronics, real-time data display, and data storage functions. Lithium-ion rechargeable batteries power the instrument for over 8 hours.

Field Use: In operation, upon connection of the LISST-SL sensor to the TCB and application of battery power, the instrumentimmediately begins isokinetic pump control, and transmission of data to the TCB. The TCB reads the data, applies built-in calibration factors, and displays velocity, SSC, mean particle size, temperature, depth, state of the battery, and pump drive parameters on an LCD screen.

Before acquiring field data, a clean water background file is required. This is a measurement of the light falling on ring detectors with clear water in the test passage. The background is acquired with the LISST-SL submerged in river water, with a 0.2 μm filter on the intake, and waiting long enough to reach thermal equilibrium. After acquisition of this background, the instrument can be raised or lowered at will. Data are continuously transmitted as averages of 16 scans of the detector rings, at approximately 2 sec intervals.

The instrument weighs 16kg in air, and about 7kg in water. Large tail fins below the main body orient the instrument into river flow immediately after touching the water surface. Because depth is sensed by a pressure sensor, wire angle does not affect accuracy of depth measurement, though practical considerations, e.g. loss of visibility of the instrument as it drifts under a bridge deck, require limiting wire angles by added weight. After stopping data collection, data are offloaded to a PC. Data processing requires the background file, the data file, and a factory background file that permits correction for any drift in laser output.

Site Description

Measurements were made from a bridge on the Cowlitz River, in the town of Castle Rock, Washington USA. The bridge is located at coordinates 46^{o} 16' 28.46"N and 122^{o} 54' 48.43"W. The Cowlitz river flows N-S, Fig. 3 after a bend and after it merges with the Toutle river that drains Mt Saint Helens. The river has a 750m long, straight run upstream of the bridge,. The river width at the bridge is 81 m, depth is 4m. This depth to width ratio suggests that the flow would closely approximate a one-dimensional channel flow. Sand movement as bedload transport was evident from depth measurements. Large turbulent boils of order 10m diameter were common at the surface, with visibly varying sediment concentrations. Water temperature was 6.7^{o}C

throughout the water column. The Bieden Group (2010) has provided extensive long-term data on sediment and water discharge in the Cowlitz river.

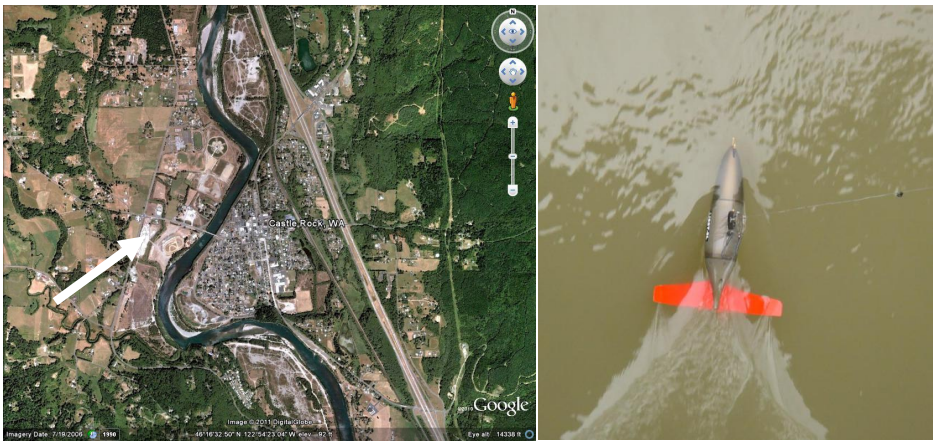

Figure. 3: Cowlitz River, the bridge, and the LISST-SL suspended from a bridge, in a river (viewed from bridge).

Data

During the day on 15 March 2011, data were acquired in many modes – fixed point time series, vertically spaced time series, and in 'integrating' mode where the LISST-SL was continuously lowered and raised in a manner similar to isokinetic bottle samplers. A total of 8 data files in various modes were

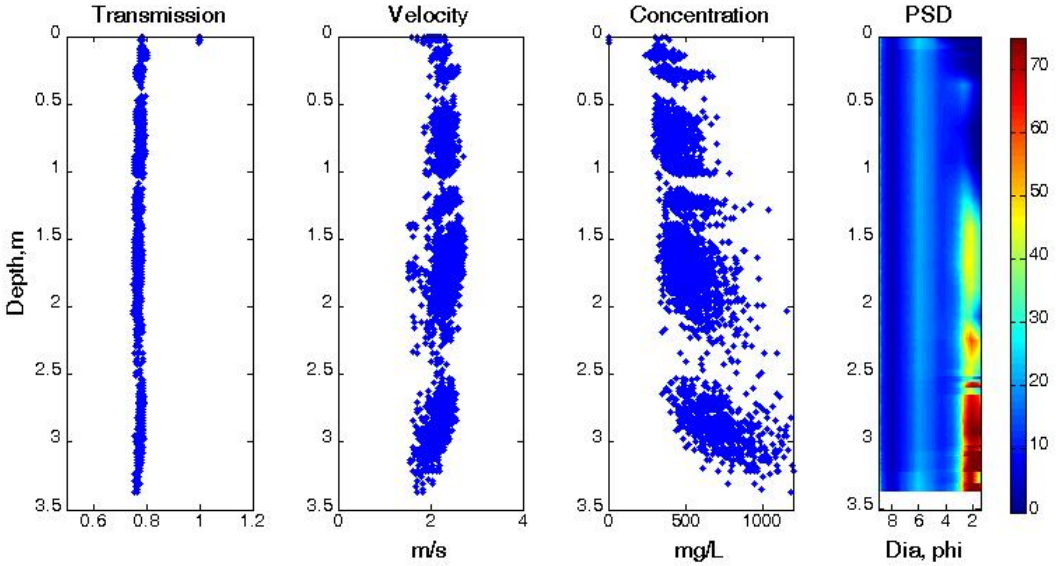

Figure 4: The raw recorded data in one profile. In the optical transmission profile, clear water background calibration points are seen at the surface with transmission of 1.0, and corresponding concentration of 0 is visible at the top of the concentration profile.

saved over 4 hours. The data included a total of 3,640 points in the profile, with pauses and interruptions. We have found it suitable to combine them all

into one long time series. Since the river flow is expected to be statistically stationary over periods of a few hours, this appears reasonable, as the data also show.

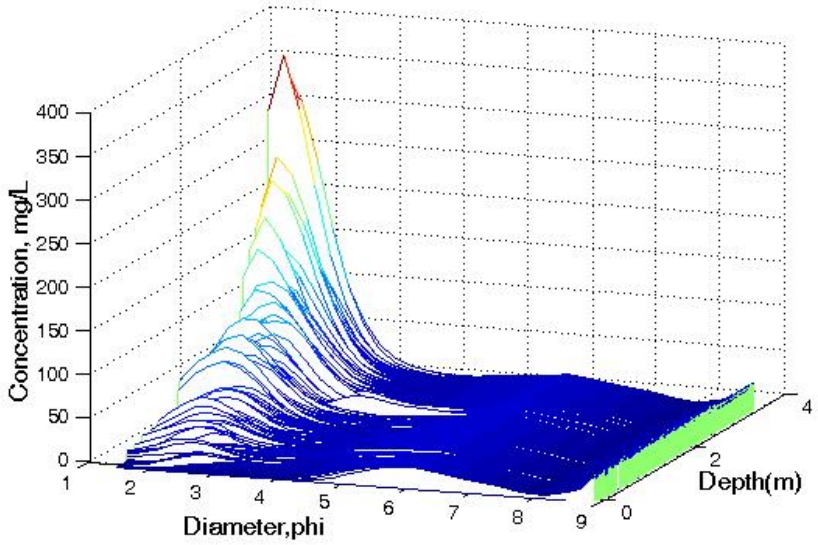

Figure 5: Size Distribution of suspended particles in a vertical profile displays a constant mode a phi value of about 5, and a rising mode with depth, centered around a phi value of 1.

From Fig. 4a, it is seen that the optical transmission is almost constant at 78% with very little vertical gradient. Optical transmission depends on total particle area concentration, so the implication is that area concentration is not changing in a significant way. This is similar to the uniform turbidity reported by Laguionie et al.(2007). The velocity profile (Fig.4 b) shows a nearly constant upper part with velocities around 2.1 m/s down to a depth of 2.5 m,

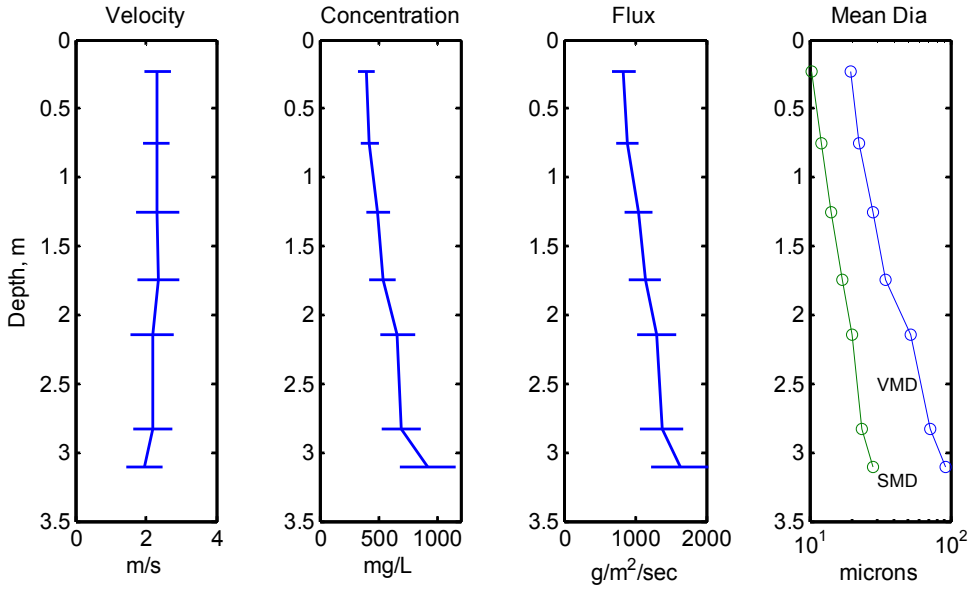

Figure 6: Mean ± one standard deviation of the profile. Note SMD is magnified 5x. Note also, the logarithmic size scale in the last panel.

and then a slight decrease to 1.8 m/s approaching bottom. The SSC profile (estimated from LD,Fig. 4c) shows a fairly distinct edge on the left at all depths, suggesting that there is a well-defined minimum concentration of 300 mg/l throughout most of the profile, though this minimum loses definition nearest the bed. The total SSC shows a steady increasing trend approaching

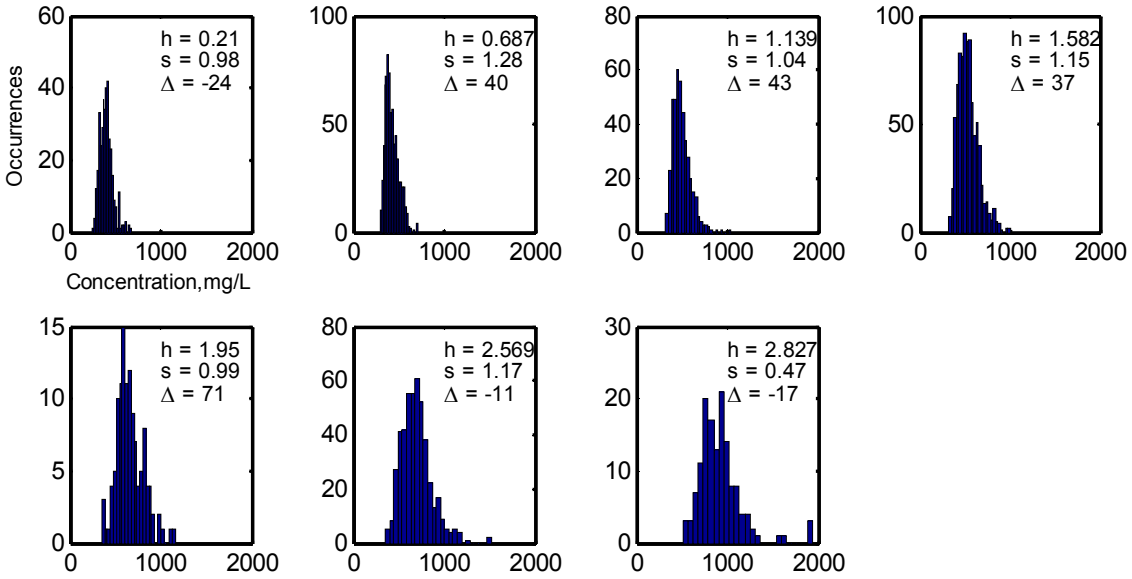

Figure 7: Histograms of sediment concentration, depths 0:5:0.5:3.5m (left to right, top to bottom). Depth is shown as h (m), and the skewness of each distribution is shown as s on each plot. The bias, i.e. difference of mean and most frequent occurrence is shown as Δ mg/L

bottom. This increase might be seen to be in apparent contradiction with the nearly invariant optical transmission data, but as we show next, this is due to the increasing presence of coarser grains nearer the bed. Note that at any given depth, the SSC exhibits a variation by a factor of 2-3, although the variation in optical transmission is insignificant. The size distribution profile as a function of depth is displayed in Fig.4d. It can be seen that a constant mode centered at 6ϕ exists at all depths, and then a coarse mode, centered around 2ϕ appears to grow stronger and shifting toward coarser sizes, approaching bottom. The fine mode (centered at 6ϕ) also explains the defined minimum concentration at all depths –coarse particles only add to it. This explains the near-constant vertical profile of optical transmission in our data, and possibly also in the turbidity data of Laguionie et al.(2007).

The size distribution data of Fig. 4d is more obvious when seen in Fig. 5. This shows more clearly that a fine mode is well mixed through the water column, but a coarse mode grows as water depth increases. The shift in this mode toward coarser particles with a diameter of ~1ϕ with depth is also clearer.

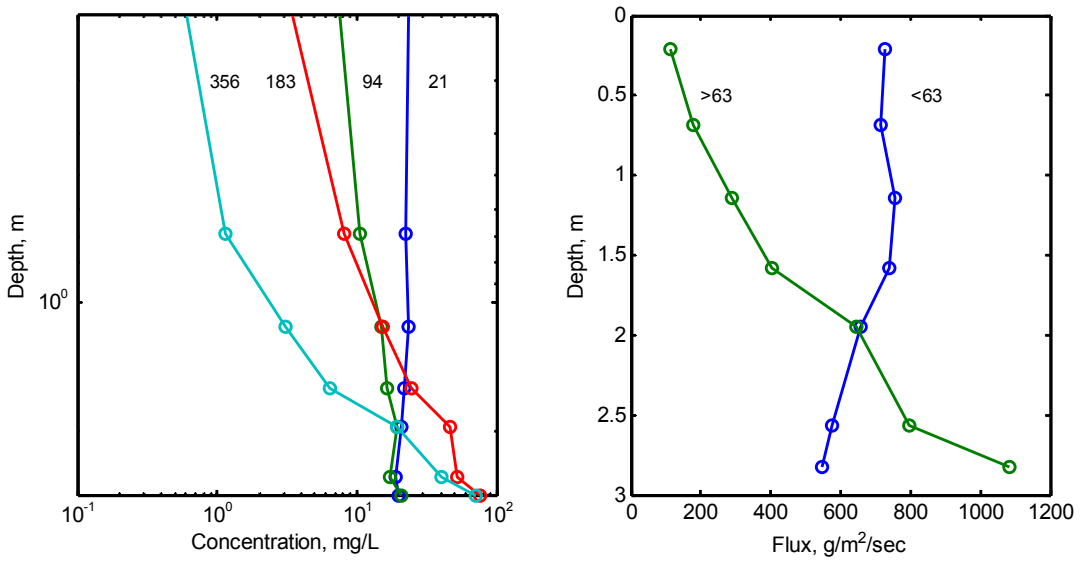

Figure 8: (*left*) concentration profile of 4 different particle sizes (numbers are sizes in microns; note the well-mixed 21 μm size mode) ; and (*right*) flux of fine (<63) vs coarse fractions (>63 microns).

The data of Fig. 4 are binned into 0.5m depths and plotted as averages in Fig.6. Now, the vertical structure emerges more clearly. Velocity, mostly constant, suggests a decrease approaching the riverbed. Concentration increases by a factor of about 3 approaching bottom, and even so, it is not noticeable in the optical transmission record of Fig.4, The sediment flux also increases strongly near the bed, from 0.8 kg/m^2/s at the surface to 1.7 kg/m^2/s near the bed. The coarsening of the size distribution approaching bed is

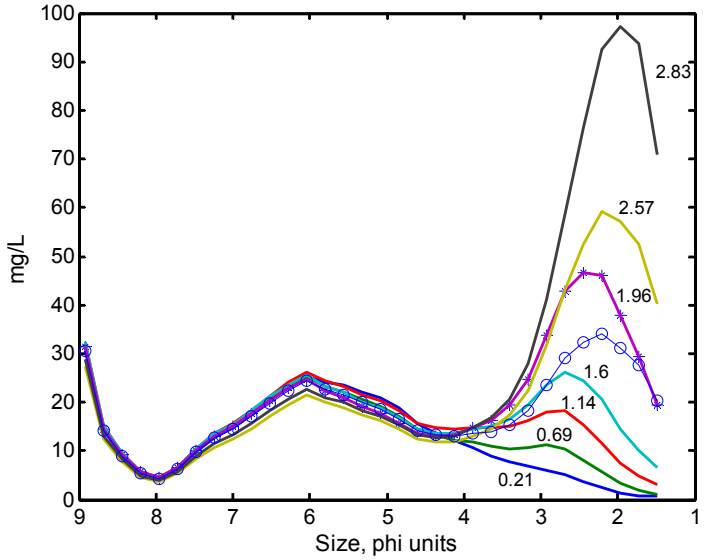

Figure 9: The mean PSD's at all 7 depths (solid lines); the profile-mean PSD (-o-), and the PSD at half-depth (-*-). Numbers on curves are depth in m.

revealed very dramatically in the last panel of Fig.6. The volume-mean particle diameter (VMD) is seen to increase by a factor of ~ 5 from 20 to 100 μm. Similarly also shown is the Sauter Mean Diameter (SMD), the ratio of particle volume concentration to area concentration. A change in SMD implies

a direct change in calibration of area-based, turbidity or transmission type sensors. The SMD is seen to change by a factor of 2.5 from top to bottom; from 10 to 25 μm. In other words, an area based sensor such as the transmissometer or an OBS or other turbidity sensor would change its calibration by 250% over such a size change. This observation alone emphasizes the need to pay close attention to size variation over just a depth of 3.5 meters in this water column.

Discussion

The LISST-SL generates rich hydrodynamic and sediment data. All parameters – velocity, depth, optical transmission, multi-angle laser scattering, and temperature were saved simultaneously in a single record every 2 seconds. Each 2-second sample involved the average of 16 scans of the ring-detectors, so that the size distribution constructed from it represents roughly a volume
defined by the 6mm intake diameter and ~ 4m of water ingested, i.e. order 100 mL, i.e. each size distribution is averaged over a horizontal cylinder 6mm x 4m long. Velocity, however, is read only once every 2 seconds, not averaged. Thus the time resolution in velocity measurement is not sufficient to construct turbulence spectra out to inertial wave-numbers, which might provide estimates of kinetic energy dissipation rates and the friction velocity. Even so, regular sampling of a quasi-random process (such as the passage of turbulent eddies) can be shown to produce unbiased variances, provided the length of duration is sufficient. This duration must be several integral time-scales of turbulence. This timescale is the ratio of depth of water divided by mean velocity, i.e. about 2 seconds in this case. Each of the velocity samples can therefore be considered statistically independent, and the variances to be accurate at each depth (typically 500 data points), with estimation errors in the mean of order $\sigma_v/N^{1/2}$ where N is the number of samples since each is statistically independent. Consequently, the mean velocities have small estimation errors of order 5 cm/s. The large spread of concentration nearer the riverbed is particularly exaggerated at the lowest samples, where a 3:1 variation in concentration is noticeable (Fig.4c). This prompts the question: how accurate would be a sample taken by a sampler such as the USGS-P63[3]?

Looking at the histograms of SSC, Fig. 7, it is seen that they are not symmetric, and certainly not Gaussian. The distributions are right-skewed. The skewness arises from the presence of a minimum concentration which, as noted, is the well-mixed washload mode centered at 6ϕ (Fig.4d). The histograms show that the most likely concentration is not the mean, it is in fact less than the mean, and that the bias can be ~10% near the surface, but not significant near the bed (~1%). Whether or not a sampler obtains a representative sample depends again on the number of integral time scales of concentration fluctuations within the capture time. We leave this for a future discussion except to note that given integral time scales of order ~2 seconds and samplers fill times of ~10 seconds, measurements of SSC may be biased

[3] http://water.usgs.gov/fisp/products/4102003.html

toward a value that is low. These differences between most likely and mean values at each depth are shown in each frame of Fig.7.

Since the LISST-SL delivers profiles of not only the SSC but the SSC in each of the 32 size classes, it is logical to examine how well the SSC profiles for each size class fits the Rouse profile. The Rouse(1937) formula for the vertical dependence of concentration can be simplified to:

$$C(z) = C(z_0)\,(H\text{-}z/z_0)^{ku_*/w_f} \qquad (1)$$

where H is water depth, z is distance from the river bed, z_o is a roughness scale, w_f is the size-dependent fall velocity, k is von Karmann's constant and u_* is the friction velocity, $u_* = (\tau/\rho)^{1/2}$, τ and ρ being, respectively, bed shear stress and water density.

To investigate consistency with Rouse, we display first the profiles of a few size classes. We have chosen the well mixed mode size, 21 μm, and those with clear vertical gradients, 94, 183, and 356 μm, Fig. 8. It is seen that whereas the concentration of the fine size (21 μm) is essentially constant through out the water column, the coarser particles show a gradient that grows with grain size.

To estimate friction velocity, we rewrite Eq.1 in the form:

$$\log(C_1)\text{-}\log(C_2) = [k\,u_*/w_f]\,\log(H\text{-}z_1/H\text{-}z_2) \qquad (2)$$

from which,

$$u_* = w_f/k\,[\log(C_1)\text{-}\log(C_2)]/\log(H\text{-}z_1/H\text{-}z_2) \qquad (3)$$

We use Eq.3 to estimate the friction velocities using slopes from the relatively straight 0.5-2m parts of profiles (cf Fig.8a) for all size classes from 131 μm to 356μm. Each size class is 18% larger than the last (roughly ¼ ϕ), The derived friction velocities from different size classes are displayed in Table 1. The

Table I

Size Class no.	26	27	28	29	30	31	32
Dia. μm	131	155	183	216	255	302	352
u_* cm/sec	5.2	5.2	5.3	5.6	6.1	6.9	8.3

consistency of friction velocity estimates, and therefore by implication, the profles of concentrations of different sizes contrasts with the one to two orders of magnitude difference between observations and models in Orton and Kineke's data (Fig.3). Our estimates of friction velocities derived from sediment concentrations are consistent with the values derived by these authors from assumed bottom friction coefficients in the range of 2.2×10^{-3} to 3×10^{-3}.

While considering Rouse profies, one needs to be cautious about density stratification of the water column. We have computed the gradient Richardson number for the most serious case – nearest bottom. The estimated value is 0.012, so that stratification is not significant in this data set.

A second estimate of friction velocity is made from the river depth and gradient through the equation $u^* = (D^*I^*g)^{1/2}$, where D is river depth and I is river gradient. Using a u^* value of 0.06 m/s, D of 4 m and solving for I yields a gradient of ~1×10^{-4} or 1 cm/km. This contrasts with a mean value of 3×10^{-4} reported by USGS (2012). The present purpose is to investigate approximate consistency.

The friction velocity estimates were made assuming a mass density of the suspended particles of 2.65 g/cm^3. In reality, some unknown amount of the suspended particles might be expected to be flocculated. This would affect the estimates of u^*, as well as the SSC estimates from the LISST-SL itself. Since no SSC samples were obtained during the field work, it is difficult to directly quantify if the particles were flocculated to any large extent. However, indirectly the degree of flocculation can be qualitatively estimated using the flocculation model of Khelifa and Hill (2006). Their model computes floc density and settling velocities from the mean size of the single particles making up the flocs, and an estimate of the size of the largest floc in suspension. Based on comparisons between several thousand in situ floc settling velocity measurements and their model, Khelifa & Hill (2006) suggested input model parameters of 1 μm for the single grains and 2000 μm for the largest floc when no other information about the single grains are available. In this study the value of 1 μm for single grains was used, but a value of 650 μm for the largest particles was used instead of the 2000 μm suggested by Khelifa & Hill. The reason for this was that the PSD from the LISST-SL did not suggest the presence of any significant amount of material outside the largest size range covered by the LISST-SL (400 μm). Using these values, the Khelifa & Hill (2006) model produced estimates of the effective density and settling velocity of the suspended particles in all 32 size classes of the LISST-SL. Subsequently a friction velocity for the flocculated material, u_{floc}^*, was computed using the settling velocities from the model. The average river gradient I was then computed using u_{floc}^* for size classes 26-32. This gave a gradient of 2.4×10^{-8} , which is 4 orders of magnitude lower than the actual gradient of 3×10^{-4}. These results strongly suggest that the suspended particles were not flocculated to any large extent and that the LISST-SL largely measured the size distribution and PSD of individual sediment grains.

The sedimentologist often wishes to measure the total sediment flux through a river, and partition it into the washload and the resuspended load. This is clearly possible using the LISST-SL data. Instead of providing the flux for each of the 32 size classes, the simpler view in Fig.8b, distinguishes the washload from resuspended load. They cross at approximately half-depth in this case.

We examine next the depth where the velocity or concentration in a river channel may be representative of the mean over the depth. The velocity profile of Fig.4b is flat, suggesting that a measurement at half depth is appropriate. The small missing portion of the velocity profile near the bed is unlikely to change this conclusion significantly. The column-mean concentration of 587mg/L is seen at a depth of approximately 1.7m, also a little shallower than half-depth. If the higher concentration nearer the bed is included, the mean concentration may come closer to half depth.

The final question is: is the column mean PSD same as the PSD at half-depth? This is not the case, as shown in Fig. 9. The mean PSD has less coarse material than PSD at half-depth. This follows from the Rouse distribution, where the coarse sediment concentration decays exponentially away from the riverbed.

Conclusion

Detailed water column data on velocity, particle size distribution, optical transmission, temperature, and depth observed with the new LISST-SL instrument reveal: Concentrations at a fixed depth can vary by a factor of 2 and even higher. The histogram of SSC samples is skewed right, indicating that traditional sampling methods will underestimate actual SSC, in this case up to 10%. The suspended sediment concentration increases toward the river bed by a factor of 3 in the present observations, though a turbidity type sensor would have missed this entirely due to the 2.5 factor increase in SMD. The vertical gradient in concentration is steepest for the coarsest grains. Vertical gradients of the coarsest grains yield fairly consistent estimates of friction velocities of ~ 6 cm/s in the mid water column. The volume mean grain size is shown to increase 5-fold towards the bed, from 20 to 93 microns. In this particular location on the river, the data also shows that the mean current velocity and SSC can be appropriately estimated by a measurement at half depth, whereas the mean particle size distribution cannot. Finally, turbidity sensors or acoustic sensors need to be used carefully in these environments due to changing grain size.

Acknowledgements

The data presented in this paper were acquired by Christopher Curran and Raegan Huffman of United States Geological Survey (USGS), Tacoma, Washington. The instrument used for this study is undergoing testing at USGS at the time of this writing. The analysis was supported by internal R&D funding of Sequoia Scientific, Inc.

References

Agrawal, Y.C., and H.C. Pottsmith, 2000: Instruments for Particle Size and Settling Velocity Observations in Sediment Transport, Marine Geology v168/1-4, pp 89-114

Agrawal, Y.C., Amanda Whitmire, Ole A. Mikkelsen and H.C. Pottsmith, 2008: Light Scattering by Random Shaped Particles and Consequences on Measuring Suspended Sediments by Laser Diffraction; J. Geophys. Res., 113, C04023, doi:10.1029/2007JC004403

Sutherland T.F., Lane P.M., Amos C.L., J. Downing**,** 2000**: "**The calibration of optical backscatter sensors for suspended sediment of varying darkness levels", Marine Geology, v 102, pp 587-607

Thorne, P.D., and D.M. Hanes, 2002: A review of acoustic measurement of small-scale sediment processes, Continental Shelf Res. V22, pp603-622.

Kazimierz, B. A.J. Horowitz, P.N. Owens, M. Stone and D.E. Walling,(2010) (eds.) IAHS Publication 337, *ISBN 978-1-907161-10-0, 376pp.*

Khelifa, A., and Hill, P.S. (2006): Models for effective density and settling velocity of flocs. Journal of Hydraulic Research 44, pp 390-401.

Languione, P., A. Crave and A. Jigore, 2007: Velocity and suspended sediment concentratin profiles in rivers: in situ measurements and flux modeling, River Basin Management IV, 335., WIT Transactions on Ecology and the Environment, v 104, pp335-343.

Nilsson, B., 1969: Development of a depth-integrating water sampler**.** *UNGI Rapport* 2, 17 pp.
Uppsala University, Department of Physical Geography, ISSN 0375-8109.

Orton, P.M. and G.C. Kineke, 2001: Comparing calculated and observed vertical suspended-sediment distributions from a Hudson river estuary turbidity maximum, Estuarine, Coastal and Shelf Science, v 52, pp 401-410.

Parsons, J.S., R.E. Goodson, and F.R> Goldschmied,1974: J. Hydronautics, v8,n3, pp 100-107.

Richey, J.E., R.H. Meade, E.Salati, A.H.Devol,C.F.Nordin, and U.D. Santos, 1986: Water discharge and suspended sediment concentrations in the Amazon River: 1982-1984; Water Resources Res. V22,n5, pp 756-764.

Rouse, H. 1937 Modern conceptions of the mechanics of fluid turbulence. *Transactions of the American Society of Civil Engineers;* **102,** 463–541

Schlichting, H., 1968: Boundary Layer Theory, McGraw Hill, New York.

Sutherland T.F., Lane P.M., Amos C.L., J. Downing, 2000: “The calibration of optical backscatter sensors for suspended sediment of varying darkness levels”, Marine Geology, v 102, pp 587-607

The Biedenharn Group, 2010: Toutle/Cowlitz River Sediment Budget, un-numbered Report prepared for the US Army Corps of Engineers, Portland District, OR, USA.

USGS, 2012: Priority Gaging Stations. Available from http://vulcan.wr.usgs.gov/Projects/Sediment_Trans/PP1573/HTMLReport/PP1573.4.html. Accessed 13 April 2012.